Aalborg Universitet

AALBORG UNIVERSITY
DENMARK

Low Voltage Ride-Through of Single-Phase Transformerless Photovoltaic Inverters

Yang, Yongheng; Blaabjerg, Frede; Wang, Huai

Published in:
IEEE Transactions on Industry Applications

DOI (link to publication from Publisher):
10.1109/TIA.2013.2282966

Publication date:
2014

Document Version
Early version, also known as pre-print

Link to publication from Aalborg University

Citation for published version (APA):
Yang, Y., Blaabjerg, F., & Wang, H. (2014). Low Voltage Ride-Through of Single-Phase Transformerless Photovoltaic Inverters. *IEEE Transactions on Industry Applications*, *50*(3), 1942-1952. https://doi.org/10.1109/TIA.2013.2282966

General rights
Copyright and moral rights for the publications made accessible in the public portal are retained by the authors and/or other copyright owners and it is a condition of accessing publications that users recognise and abide by the legal requirements associated with these rights.

- Users may download and print one copy of any publication from the public portal for the purpose of private study or research.
- You may not further distribute the material or use it for any profit-making activity or commercial gain
- You may freely distribute the URL identifying the publication in the public portal -

Take down policy
If you believe that this document breaches copyright please contact us at vbn@aub.aau.dk providing details, and we will remove access to the work immediately and investigate your claim.

Downloaded from vbn.aau.dk on: April 20, 2024

© 2013 IEEE. Personal use of this material is permitted. Permission from IEEE must be obtained for all other uses, in any current or future media, including reprinting/republishing this material for advertising or promotional purposes, creating new collective works, for resale or redistribution to servers or lists, or reuse of any copyrighted component of this work in other works.

Digital Object Identifier (DOI): 10.1109/TIA.2013.2282966

IEEE Transactions on Industry Applications, in press, online available on 20 September 2013

Low Voltage Ride-Through of Single-Phase Transformerless Photovoltaic Inverters

Yongheng Yang
Frede Blaabjerg
Huai Wang

Suggested Citation

Y. Yang, F. Blaabjerg, and H. Wang "Low voltage ride-through of single-phase transformerless photovoltaic inverters," *IEEE Trans. Industry Applications,* in press.

Low Voltage Ride-Through of Single-Phase Transformerless Photovoltaic Inverters

Yongheng Yang, *Student Member*, *IEEE*, Frede Blaabjerg, *Fellow*, *IEEE*, and Huai Wang, *Member, IEEE*

***Abstract* – Transformerless photovoltaic (PV) inverters are going to be more widely adopted in order to achieve high efficiency, as the penetration level of PV systems is continuously booming. However, problems may arise in highly PV-integrated distribution systems. For example, a sudden stoppage of all PV systems due to anti-islanding protection may contribute to grid disturbances. Thus, standards featuring with ancillary services for the next generation PV systems are under a revision in some countries. The future PV systems have to provide a full range of services as what the conventional power plants do, e.g. Low Voltage Ride-Through (LVRT) under grid faults and grid support service. In order to map future challenges, the LVRT capability of three mainstream single-phase transformerless PV inverters under grid faults are explored in this paper. Control strategies with reactive power injection are also discussed. The selected inverters are the full-bridge inverter with bipolar modulation, the full-bridge inverter with DC bypass and the Highly Efficient and Reliable Inverter Concept (HERIC). A 1 kW single-phase grid-connected PV system is analyzed to verify the discussions. The tests confirmed that, although the HERIC inverter is the best candidate in terms of efficiency, it is not very special feasible in case of a voltage sag. The other two topologies are capable of providing reactive current during LVRT. A benchmarking of those inverters is also provided in this paper, which offers the possibility to select appropriate devices and to further optimize the transformerless system.**

***Index Terms* – Low voltage ride-through, grid support, single-phase systems, photovoltaic (PV), transformerless inverters, reactive power injection, efficiency, leakage current elimination.**

I. Introduction

THE YEAR of 2012 has been another year for an extraordinary growth of photovoltaic (PV) systems with total global operating capacity reaching the 100 GW milestone [1]. However, this high penetration level of PV systems may also introduce negative impacts on the grid. Concerns like power quality issues, the efficiency and the emerging reliability are becoming of high interest and intense importance [2]-[9]. Thus, many grid codes have been released to regulate PV systems integration with the distributed grid [10]-[20]. Since PV systems are typically connected to low-voltage and/or medium-voltage distributed networks, the grid standards are mainly focused on power quality issues, frequency stability and voltage stability [13]. It is required that PV systems should cease to energizing local loads in presence of a grid fault, e.g. a voltage sag and a frequency disturbance [13], [17], which is known as an anti-islanding protection.

Due to the still declined PV cell price and the advanced power electronics technology, the penetration degree is going to be much higher. In view of this, the impact of highly penetrated PV systems, even serving low-voltage networks, on the grid cannot be neglected anymore. A sudden stoppage of all grid-connected PV systems in an unintentional islanding operation mode could trigger much more severe grid problems than the initial event, e.g. power outages and voltage flickers [2], [10], [21]. In order to solve the potential issues, several European countries have updated the grid codes for low- or medium-voltage systems. The next generation PV systems have to provide a full range of services as what the conventional power plants do. For instance, the German grid code requires that the generation systems connected to the medium- or high-voltage networks should have LVRT capability under grid faults [12], [17]. In the new Italian grid code, the generation units connected to low-voltage grid with the nominal power exceeding 6 kW have to ride through grid voltage faults [18]. Other countries like Japan [19]-[22] are undertaking a revision of their current active grid standards in order to accept more PV energy in the line. However, some standard committees, e.g. IEEE Standard Committee, still have some catching up to do [23].

Besides the ancillary services, achieving high efficiency and high reliability are always required in PV systems in order to reduce energy losses and extend service time [3], [7], [8], [24]. Compared to conventional PV systems, transformerless systems are increasing in popularity, especially in European markets, because of the high efficiency [13], [25]-[35]. Many transformerless topologies are derived by adding extra power devices into the Full-Bridge (FB) inverter. For example, the FB inverter with DC bypass (FB-DCBP) adds two power devices at the DC-side [26], [27]; while the HERIC topology provides an AC bypass leg [29]. Considering the fast growth of grid-connected PV systems, it is better for the next generation

Manuscript received July 3, 2013; revised September 2, 2013; accepted September 6, 2013. Paper 2013-IPCC-572.R1, presented at the 2013 IEEE Energy Conversion and Exposition, Denver, CO, USA, September 15-19, and approved for publication in the IEEE Transactions on Industry Applications by the Industrial Power Converter Committee of the IEEE Industry Applications Society.

Y. Yang, F. Blaabjerg, and H. Wang are with the Department of Energy Technology, Aalborg University, DK-9220 Aalborg East, Denmark. (e-mail: yoy@et.aau.dk; fbl@et.aau.dk; hwa@et.aau.dk).

Color versions of one or more of the figures in this paper are available online at http://ieeexplore.ieee.org.

Digital Object Identifier

transformerless PV inverters to equip with LVRT capability in order to fulfill the upcoming requirements efficiently and reliably.

Current stresses, power losses on the switching devices and dynamic responses of transformerless inverters are dependent on the topology configuration in both normal operation and LVRT operation mode. Thus, it is necessary to explore the performance of these PV systems under different conditions. In this paper, three transformerless PV inverters – FB inverter with bipolar modulation (FB-Bipolar), FB-DCBP inverter and the HERIC inverter are studied in terms of current stresses, efficiency, and LVRT capability with reactive power injection. Firstly, a brief introduction of the selected inverters is given. Then, the focus is shifted to the control of transformerless PV systems under grid faults. Control strategies and reactive power injection possibilities for single-phase PV systems are discussed in § III. Simulation results of LVRT operation examples are demonstrated in § IV, as well as experimental tests of a FB inverter system. A benchmarking of the selected inverters mainly in terms of leakage current elimination, LVRT capability and efficiency is presented before the conclusions.

II. Single-Phase Transformerless PV Inverters

Underpinned by the advanced and dedicated control methods, the PV inverters are responsible for converting DC source generated from PV panels to AC source efficiently and reliably. A widely adopted single-phase PV inverter is the FB topology as shown in Fig. 1, where it is connected to the grid through an *LCL*-filter in order to ensure the injected current quality. There are two main modulation strategies available for this inverter: a) unipolar modulation scheme and b) bipolar modulation scheme.

When the transformer is removed from a grid-connected PV system, safety concerns (e.g. leakage current) will arise since the lack of galvanic isolations. Thus, transformerless inverters should eliminate or at least reduce the leakage current, e.g. by including passive damping components and/or by modifying the modulations [26]. In the light of this, the FB-Bipolar is more feasible in single-phase transformerless PV applications. However, in every switching period, there are reactive power exchange between the *LCL*-filter and the capacitor C_{PV} and also core losses in the output *LCL*-filter, leading to a low efficiency of up to 96.5% [13].

In order to further improve the efficiency and reduce the leakage current, a tremendous number of transformerless topologies have been developed [13], [25]-[35], most of which are based on the FB inverter as it is shown in Fig. 1. As aforementioned, the first priority of a transformerless inverter is to avoid the generation of a varying instantaneous Common-Mode Voltage (CMV, v_{CMV}), since the CMV will induce a common-mode current (leakage current). The relationships can simply be described as,

$$v_{CMV} = \frac{v_{AO} + v_{BO}}{2}, \tag{1}$$

$$i_{CMV} = C_P \frac{dv_{CMV}}{dt}, \tag{2}$$

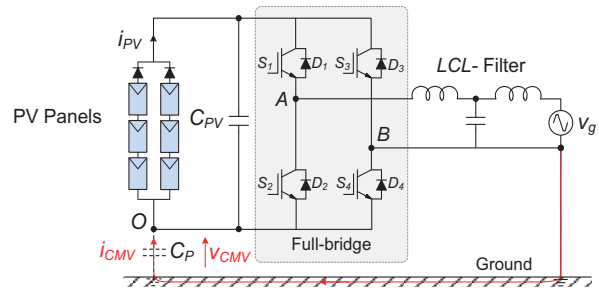

Fig. 1. A single-phase Full-Bridge (FB) grid-connected PV system with an *LCL*-filter.

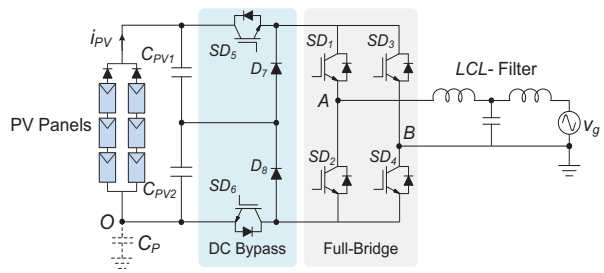

(a) Full-bridge with DC bypass topology [26], [27]

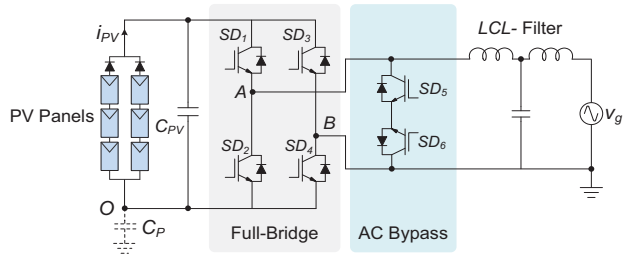

(b) Highly efficient and reliable inverter concept, HERIC [29]

Fig. 2. Two main grid-connected transformerless PV systems with *LCL*-filter (*SD*-IGBT module, *S*-IGBT, *D*-Diode).

where v_{AO} and v_{BO} are the voltages of the two midpoints of a FB inverter shown in Fig. 1, i_{CMV} is the common-mode current, and C_P is the stray capacitor between PV panels and the ground.

Besides those solutions to limit the leakage current by adding passive damping components and by modifying the modulation techniques, the elimination can also be achieved either by disconnecting the PV panels from the inverter or by providing a bypass leg at the AC side. For instance, the FB-DCBP inverter patented by Ingeteam [26], [27] shown in Fig. 2(a) disconnects the PV panels from the inverter using four extra devices (two switching devices SD_5, SD_6 and two diodes D_7, D_8); while the HERIC inverter (Fig. 2(b)) by Sunways [29] provides an AC bypass using two extra switching devices (SD_5, SD_6). There have been other transformerless topologies reported in the literature. Some are based on the multi-level topologies [31]-[33], and some are derived by optimizing traditional transformerless inverters [34], [35].

In respect to the modulation of a transformerless inverter, it should not generate a varying CMV. With a dedicated modulation scheme for those inverters, there is no reactive power exchange between the *LCL*-filter and the capacitor C_{PV} at zero-voltage states, and thus higher efficiency is achieved. However, extra power losses, including switching losses and conduction losses, will appear on the required additional

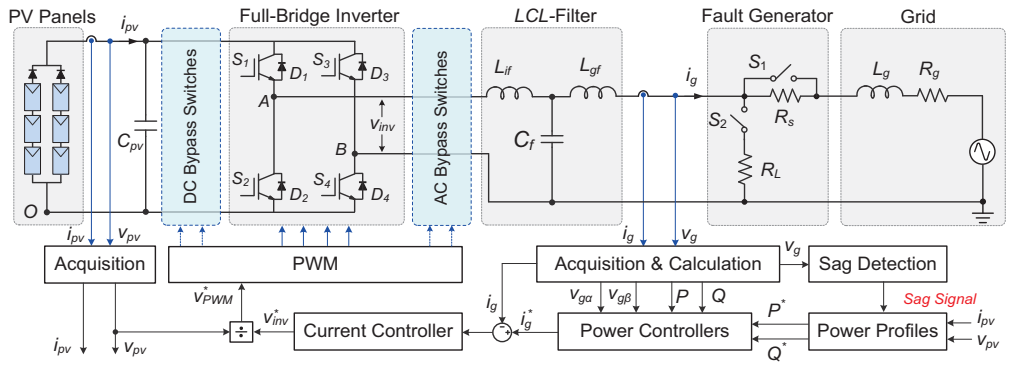

Fig. 3. Hardware schematic and control diagram of single-phase transformerless grid-connected PV systems with low voltage ride-through capability.

switching devices in these inverters as shown in Fig. 2. Moreover, the power losses of an individual switching device are dependent on its commutation frequency, which differs with inverter topologies, and its electrical stress. For example, the extra devices, S_5 and S_6 in the FB-DCBP inverter are commutated at a high switching frequency (e.g., 10 kHz); while those in the HERIC inverter commutate at the line fundamental frequency (e.g., 50 Hz). Since the total power losses will further introduce redistributions of both current and thermal stresses on the devices among these inverters, the efficiency and the lifetime will be affected [3], [7].

Concerning LVRT operation, the control systems and the dynamic response of the above inverters possibly differ with the configurations and the modulation schemes. They may have a significant impact on the capability of reactive power injection to support the grid voltage recovery under grid faults. Moreover, the overstresses on the switching devices may also cause failures during LVRT and thus increase the maintenance cost. Those aspects should be taken into consideration for the design and operation of transformerless PV systems. Thus, essentially, this paper explores the performance of the mainstream transformerless inverters with the consideration of such operation conditions.

III. Control of Transformerless PV Inverters under Grid Faults

According to the grid requirements, the design of next generation transformerless PV systems should take into account not only the shape of grid current (power quality issues), but also the behavior of reactive power injection under grid faults. Fig. 3 shows the hardware schematic and overall control structure of a single-phase single-stage transformerless PV system with LVRT capability.

Typically, the control strategy applied to a single-phase grid-connected system includes two cascaded loops [13], [14]:

a) An inner current control loop, which has the responsibilities of power quality issues and current protection of the inverter and,

b) An outer voltage control (or power control) loop, in which the grid voltage is controlled to generate desired current references for the inner control loop.

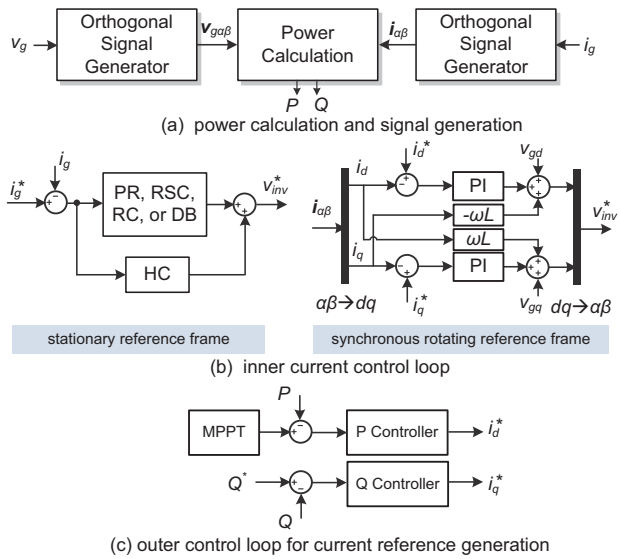

Fig. 4. Implementation of current control loop for single-phase single-stage systems in different reference frames.

A. Current Control Loop

For the current control loop, as detailed in Fig. 4, the existing control methods, such as Proportional Resonant (PR), Resonant Control (RSC), Repetitive Controller (RC), and Deadbeat Controller (DB) can be adopted directly, since they are capable to track sinusoidal signals without steady-state errors [14], [17], [36]-[39]. Further, applying the Park transformation ($\alpha\beta \rightarrow dq$) leads to the possibility of Proportional Integral (PI) controllers to regulate the injected current, and afterwards, the modulation reference v^*_{inv} can be obtained by means of the inverse Park transformation ($dq \rightarrow \alpha\beta$) [37], [40]. However, as it is shown in Fig. 4, the implementation of a PI-based current control loop in the synchronous rotating reference frame requires a signal generation system, which can produce a quadrature component corresponding to the input, and thus the complexity increases [37]. Since the current control loop is responsible for the power quality, this responsibility should also be effective and valid in the design of current controllers and also the *LCL*-filter. By introducing Harmonic Compensators (HC) for the controller [13], [14] and adding passive damping for the filter, an enhancement of the current controller tracking performance can be achieved.

Since the PR+HC controller presents a good performance in terms of accurate tracking (harmonic rejection) [13], [14], [38], [39], this controller is selected in this paper as the inner current controller. Compared to the conventional PI-based current controller in the synchronous rotating reference frame, the PR+HC controller does not require quadrature signal generator and *dq*-currents decoupling as shown in Fig. 4. The transfer function of this current controller can be given as,

$$G_i(s) = k_p + k_r \frac{s}{s^2+\omega_0^2} + \sum_{h=3,5,7} \frac{k_{rh} s}{s^2+(h\omega_0)^2}, \quad (3)$$

in which k_p is the proportional gain, k_r is the fundamental resonant control gain, k_{rh} is the control gain for h-order resonant controller ($h = 3, 5, 7$) and ω_0 is the grid fundamental frequency.

B. Voltage Control Loop (Power Control Loop)

For the outer voltage control loop, it provides the system operation conditions (e.g. grid voltage amplitude and grid frequency) and then it generates a current reference, which is subsequently utilized in the inner current control loop. Thus, it offers the possibilities to add control methods into this loop to shape the grid current in LVRT operation mode with the purpose of reactive power injection. For example, based on the single-phase *PQ* theory [9], [17], [40]-[44], the injected grid current reference can be produced by regulating the averaged active power and reactive power, as it is shown in Fig. 3 and Fig. 4. This power control method is intuitive and simple, since the averaged active power and the averaged reactive power references (P^* and Q^*) can directly be set by the operators/ control unit. With the help of orthogonal signal generator systems, the grid current reference i^*_g can be expressed as,

$$i_g^* = \frac{1}{v_{g\alpha}^2 + v_{g\beta}^2} \begin{bmatrix} v_{g\alpha} & v_{g\beta} \end{bmatrix} \begin{bmatrix} G_P(s)(P-P^*) \\ G_Q(s)(Q-Q^*) \end{bmatrix}, \quad (4)$$

where $v_{g\alpha}$, $v_{g\beta}$ are the orthogonal components of the grid voltage, respectively, P, Q are the averaged active power and reactive power, P^*, Q^* are the power references and $G_P(s)$, $G_Q(s)$ are PI-based controllers for the active power and the reactive power, respectively.

In respect to the orthogonal signal generator systems, several methods have been reported to create the corresponding quadrature signal of the grid voltage, such as the Hilbert transform based method, the inverse Park transform based method, and the Second Order Generalized Integrator (SOGI) method [9], [13], [14], [44]-[46]. Due to the advantages of simple implementation and delay-free property, the SOGI generation system is adopted in this paper according to the benchmarking results presented in [9] and [13].

There are also other control possibilities available for the outer control loop, such as the droop-based control and the instantaneous power control [37], [42], [43], [47]-[49]. The droop-based power control method is implemented based on the assumption that the distributed line is mainly inductive [47]. However, in fact, the PV systems have been dominated by

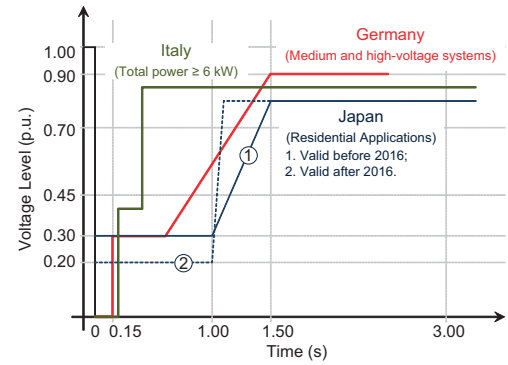

Fig. 5. Low voltage ride-through requirements defined in different countries covering a wide range of applications [9]-[12], [17]-[19].

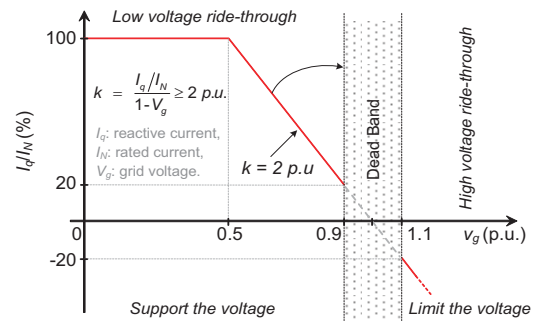

Fig. 6. Reactive current injection requirements for medium- and/or high-voltage wind turbine power systems defined in E.ON grid code [11], [12].

residential applications with low rated power and low voltage grid. In this case, such assumption is not valid. The instantaneous power control method acts directly on the instantaneous power, and subsequently the reference current is produced. Thus, there is no need to calculate the averaged active power and reactive power for this control strategy [37]. It may be a good candidate for single-phase applications in LVRT operation mode.

Nevertheless, in regard to the above control methods, e.g. the *PQ* control strategies, a fast voltage sag detection and an accurate synchronization system will strongly contribute to the dynamic performance and the stability margin of the whole control systems. Even for the instantaneous power control method, the syntheses of instantaneous power reference from the averaged active power and reactive power references is affected by the knowledge of grid conditions [37].

C. Reactive Power Injection Strategies

The "*Power Profiles*" unit in Fig. 3 is used to generate the average active power and reactive power references for the power controllers, and subsequently, the references are controlled to produce the grid current reference as discussed previously. In the normal operation mode, the average active power reference P^* is the output of a Maximum Power Point Tracking (MPPT) system, as shown in Fig. 4 and the system is required to operate at unity power factor (i.e. $Q^* = 0$ Var).

When a voltage fault is detected by the "*Sag Detection*" unit, the PV system enters into the LVRT operation. It is required by the grid codes that the system should withstand the voltage drop for a specified short period, as it is shown in Fig. 5. At the same

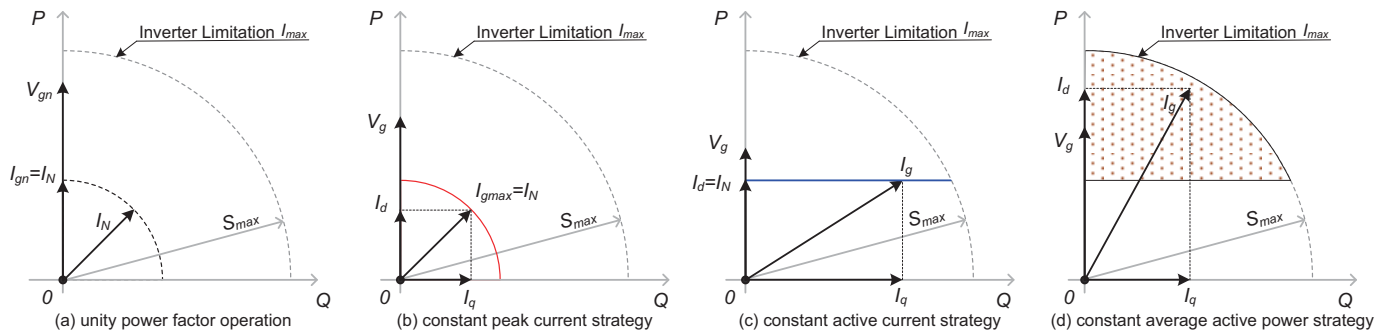

Fig. 7. Representations of the grid current and the grid voltage of a single-phase PV system with different reactive power injection strategies ($v_g \geq 0.5$ p.u.).

time, the PV system should inject reactive power (current) to support the grid voltage recovery [9], [17]-[22]. Fig. 6 shows an example of the required reactive power injection during LVRT for medium- and high-voltage wind turbine power systems specified in the German E.ON grid code. According to the requirements defined in Fig. 6, the averaged reactive power reference Q^* is a function of the grid voltage level in LVRT operation mode. Then it is controlled and injected into the grid to support the voltage recovery.

Although the LVRT demand (by German grid code) shown in Fig. 5 and Fig. 6 is initially set for medium and/or high voltage applications – wind turbine power systems, it is worth mentioning that low voltage PV systems are already on an upward track to dominate in the electricity generation [1], [2]. In this case, the LVRT demands are expected to be extended to all the PV systems even including the PV modules [9]-[11], [19]-[22]. Through reactive power injection during LVRT, the grid voltage can be stabilized and also an avoidance of PV power generation can be achieved [2], [9], [21]. Thus, the following presents the reactive injection strategies for single-phase systems, starting with an overview of possible reactive power injection strategies for three-phase applications.

For three-phase applications, the reactive power injection strategies can be summarized as: 1) unity power factor control strategy, 2) positive and negative sequence control strategy, 3) constant active power control strategy and 4) constant reactive power control strategy [13], [14], [21], [50]-[55]. Unbalanced grid conditions are more common in three-phase systems. Since there is an interaction between voltage sequences and current sequences under grid faults, either the controlled active power or the controlled reactive power will present oscillations [56]. Thus, in [56], the zero-sequence control path has been introduced to further increase the control freedoms and to eliminate the oscillations in the controlled power.

For single-phase systems, there are even less control freedoms. By considering the overcurrent protection of PV inverters and the reactive current injection requirements under grid faults, possibilities for reactive power injection of single-phase PV systems are proposed as follows:

1) Constant Peak Current Strategy

With this control strategy, there is no risk of inverter shutdown due to overcurrent protection, since the peak of the injected grid current (I_{gmax}) is kept constant during LVRT. The injected reactive current level (I_q) is calculated according to Fig. 6. The grid peak current I_{gmax} can be set as the rated current level I_N of the PV system, for example,

$$\begin{cases} I_{g\max} = I_N \\ I_q = k\left(1 - v_g\right) I_N \end{cases}, \tag{5}$$

in which v_g is the grid voltage, 0.5 p.u. $\leq v_g \leq$ 0.9 p.u., and $k \geq 2$ p.u.. According to Fig. 6, the PV inverter should generate full reactive power (I_q=I_N) when v_g < 0.5 p.u.. The phasor diagram for this control strategy is shown in Fig. 7(b), from which it can be observed that the output active power decreases (I_d<I_N and V_g<V_{gn}) during LVRT.

2) Constant Active Current Strategy

Another control possibility under LVRT operation is to keep the active current constant. For the purpose to extract as much energy from the PV panels as possible, for example, the level of active current can be controlled to be that of the rated current (I_d=I_N), as it is shown in Fig. 7(c). The injected reactive current (I_q) is proportional to the voltage sag depth in a certain voltage range (0.5 p.u. $\leq v_g \leq$ 0.9 p.u.), as it is shown in Fig. 6. With this reactive power injection strategy, the amplitude of the injected current may exceed the inverter limitation (I_{max}). In order to avoid inverter shutdown due to over-current protection, the following condition should be fulfilled during the design and the operation of a PV inverter,

$$\sqrt{1 + k^2\left(1 - v_g\right)^2} \leq \frac{I_{\max}}{I_N}, \tag{6}$$

where v_g is the grid voltage and $k \geq 2$ p.u..

Considering a pre-designed inverter with a robustness margin, $I_{max} = 1.5I_N$, and $k = 2$ p.u., it is not possible to utilize this control strategy to inject the required reactive power, since the minimum margin is 2.06 for $k = 2$ p.u.. In such a case, the PV system should also de-rate the active power output in order to generate enough reactive power. Otherwise, over-rated operations may introduce failures to the whole system and shorten the inverter serving time, and thus the maintenance cost increases.

3) Constant Average Active Power Strategy

Similar to the constant active current control strategy, a more intuitive way to maximize output energy (i.e., to deliver maximum active power) is to keep the average active power constant during LVRT. However, the required injection of reactive power might pose a risk of over-current protection with

this control strategy. Under this situation, the currents can be expressed as,

$$\begin{cases} I_d = \dfrac{1}{v_g} I_N \\ I_q = k\left(1 - v_g\right) I_N \end{cases}, \tag{7}$$

in which v_g and k are defined previously. Thus, the following constraint should be satisfied to avoid inverter shutdown due to overcurrent protection.

$$\frac{1}{v_g}\sqrt{1 + k^2\left(v_g - v_g^2\right)^2} \le \frac{I_{\max}}{I_N}. \tag{8}$$

During the design and the operation of the PV inverters, those above constraints should be considered. Especially, for the next generation PV systems, the provision of reactive power both in normal operation and under grid faults, and the requirements of LVRT will come into force in the near future. If those above aspects are not well considered, the maintenance costs and energy losses may increase.

IV. Simulation and Experimental Results

Fig. 8 presents the closed loop control system for a single-phase transformerless PV system. It is observed in Fig. 8 that an effective power calculation method in terms of fast dynamic response and accurate computation, together with an advanced synchronization unit, can contribute to the LVRT performance of the entire system. In this paper, the SOGI based Phase Locked Loop (SOGI-PLL) has been selected as the synchronization unit because of its robustness [9], [13], [14], [45]. The average power calculations are based on the Discrete Fourier Transformation (DFT). Since the DFT uses a running window to do the calculation, it naturally will introduce a delay [57]. The other parameters of the system are listed in TABLE I. A voltage fault (0.43 p.u.) is generated by switching S_1 and S_2 of the sag generator shown in Fig. 3 and the experimental setup of a FB system shown in Fig. 9. The control system has been implemented in a dSPACE DS 1103 system. A Danfoss VLT FC302 three-phase FB inverter is used, and it is configured as a single-phase FB system in the experiments. A Delta DC source is adopted, and the DC voltage is 400 V.

A. Simulation Results

Simulations are firstly tested in MATLAB using PLECS blockset for the modelling. During LVRT operation, the control system sets the reference power according to a detected voltage sag depth, and the system will start to inject reactive power into the grid once the fault is confirmed. In the cases, the voltage sag is 0.43 p.u., and thus according to Fig. 6 and Fig. 7, the average reactive power Q^* should be 490.2 Var during LVRT, and the active power P^* should be 290 W when the constant peak current control strategy is adopted. The simulation results are shown in Fig. 10 and Fig. 11.

TABLE I
Simulation and Experimental Parameters.

Normal Grid Voltage	$V_g = 230\ V$
Normal Grid Frequency	$\omega_0 = 2\pi\times 50\ rad/s$
Grid Impedance	$L_g = 2\ mH$, $R_g = 0.04\ \Omega$
Rated Power	$P_n = 1\ kW$
Switching Frequency	$f_{sw} = 10\ kHz$
LCL-Filter	$L_{if} = 3.6\ mH$, $L_{gf} = 708\ \mu H$, $C_f = 2.35\ \mu F$
Sag Generator	$R_S = 19.3\ \Omega$, $R_L = 19.9\ \Omega$
PI based Power Controllers	$k_{pp} = 1.5$, $k_{ip} = 52$ of $G_P(s)$ - active power $k_{pq} = 1$, $k_{iq} = 50$ of $G_Q(s)$ - reactive power
PR+HC Current Controller	$k_p = 20$, $k_r = 2000$, $k_{r3,5,7} = 5000$

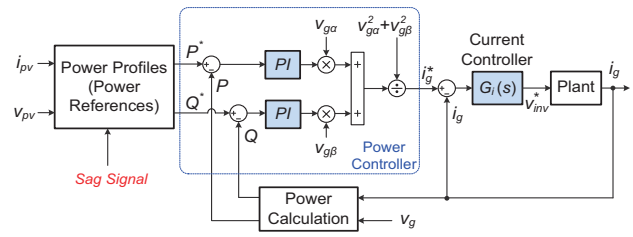

Fig. 8. Closed loop control system of a single-phase transformerless system with low voltage ride through capability based on the single-phase *PQ* theory and PR+HC current controller.

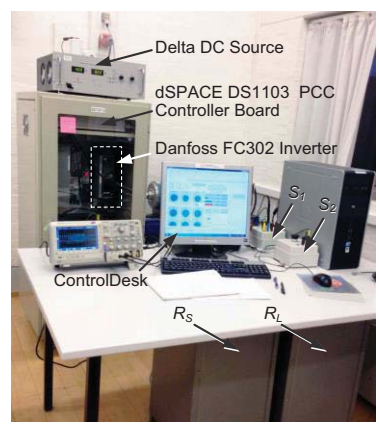

Fig. 9. Experimental setup of a single-phase full-bridge system.

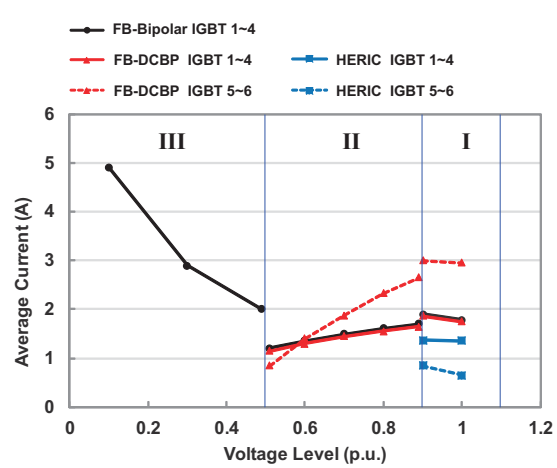

Fig. 10. Average current stresses of IGBT devices in the three transformerless PV inverters with different voltage levels: I- normal operation (0.9 p.u.$\le v_g <$ 1.1 p.u.), II-LVRT with constant peak current control (0.5 p.u.$\le v_g <$ 0.9 p.u.), and III-full reactive power injection ($v_g <$ 0.5 p.u.).

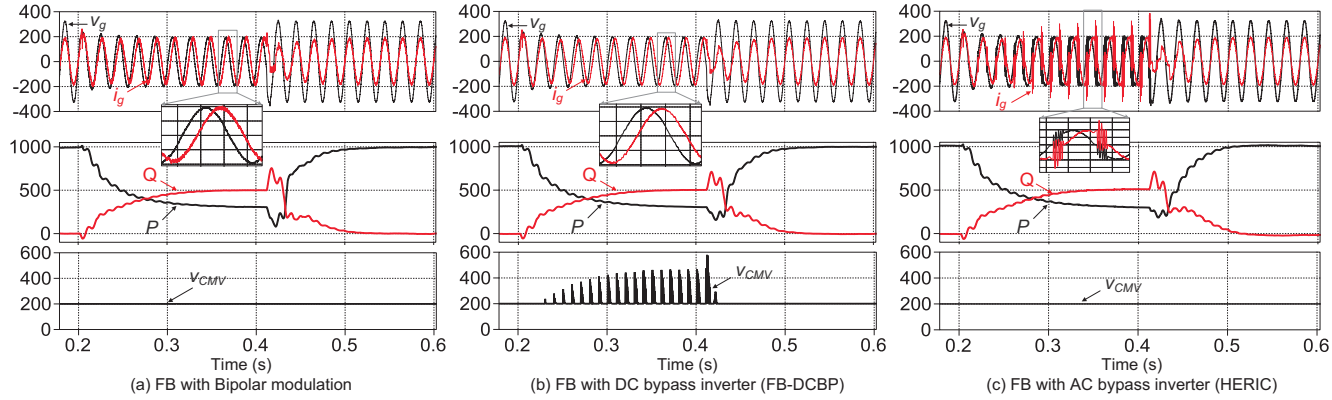

Fig. 11. Performance of the three grid-connected transformerless PV systems in low voltage ride through operation (0.43 p.u. voltage sag): grid voltage v_g [V], grid current i_g [30×A], active power P [W], reactive power Q [Var], and common mode voltage v_{CMV} [V].

TABLE II
BENCHMARKING OF THE THREE TRANSFORMERLESS INVERTERS.

	FB-Bipolar	**FB-DCBP**	**HERIC**
Number of Power Devices	Four	Six	Six
Efficiency [1]	97.61 %	97.67%	98.29%
Loss Distributions (%) [2]	$S_{1\sim4}$ 100	$S_{5\sim6}$ 52, $S_{1\sim4}$ 48	$S_{5\sim6}$ 37, $S_{1\sim4}$ 73
LVRT Capability (Reactive power injection)	YES (full range)	YES (only when grid voltage level > 0.5 p.u.)	NO (severe current distortion)
Leakage Current (CMV)	Low (CMV = *const.*)	Low (in normal operation, CMV = *const.*) High (in LVRT, CMV ≠ *const.*)	Low (CMV = *const.*)
Device Current Stresses (p.u.) [3]	$S_{1\sim4}$: 1.00	$S_{1\sim4}$: Moderate (0.98), $S_{5,6}$: Very High (1.66)	$S_{1\sim4}$: Low (0.76), $S_{5,6}$: Very Low (0.37)
Device Switching Freq. (f_s)	$S_{1\sim4}$: High f_s	$S_{1\sim4}$: Line Freq., $S_{5,6}$: High f_s	$S_{1\sim4}$: High f_s, $S_{5,6}$: Line Freq.

[1] Conversion efficiency by only considering the losses on the power devices in the normal operation mode. Rated power: 1 kW, DC voltage: 400 V.
[2] Loss distributions of the power devices in the normal operation mode (v_g = 1.0 p.u.). Percentage of the total losses on the power devices. Rated power: 3 kW.
[3] Base value - device current stresses of the FB-Bipolar. Comparison in the normal operation (v_g = 1.0 p.u.). Rated power: 1 kW, DC voltage: 400 V.

As it is shown in Fig. 10 and Fig. 11, in a wide range of grid voltage level, the FB-Bipolar inverter can provide required reactive power during LVRT operation. The FB-DCBP inverter is also capable of riding through the voltage sag within a voltage range of 0.5 p.u. to 0.9 p.u.. However, it also presents a varying v_{CMV} (high leakage current) under grid faults as shown in Fig. 11(b). Moreover, the current stresses on the extra devices of FB-DCBP are significantly higher than the four devices of a FB inverter, as it is shown in Fig. 10. The high stresses might induce failures to the whole inverter.

Since the HERIC inverter is disconnected from the grid when the transformerless inverter is also short-circuited in order to avoid leakage currents, the inverter can only operate at unity power factor (i.e. no reactive power injection capability) [13], [28]. This is implied in Fig. 11(c), in which the grid current is severely distorted at voltage zero-crossing points in LVRT operation. Considering that large current distortions will introduce more power losses, may trip the inverter overcurrent protection, and further may cause failures of the power devices, the HERIC transformerless inverter is not special suitable for use in single-phase systems in LVRT operation with reactive power injection, although the averaged powers are controlled. However, it can achieve a high efficiency among these three topologies operating at unity power factor under normal conditions, which can be observed from Fig. 10 where the current stress is shown and the benchmarking results in TABLE II. Due to the lowest current stresses on the FB devices and the extra devices, a cost-effective design can be achieved for HERIC inverter in the normal operation considering the efficiency and reliability [58].

B. Experimental Tests (FB System)

Fig. 12 and Fig. 13 show the experimental results for a single-phase FB system. It can be seen from Fig. 12 that by applying bipolar modulation strategy, the CMV of a FB inverter has been kept constant. Thus, it would not generate leakage currents. Fig. 13 demonstrates that the FB inverter is capable of riding through a low-voltage fault. It can inject the required reactive power into the grid and at the same time, the average active power generation is limited. Since the constant peak current control strategy is used in the tests, the amplitude of the grid current is kept constant during LVRT (Fig. 13(c)), which validates its effectiveness. When the voltage sag is cleared, the power control method based on the single-phase PQ theory can fast change the system to unity power factor operation, as it is shown in Fig. 13. However, due to the power calculation delay and the frequency swing, the transient current presents distortions, especially during voltage recovery. Nevertheless, those tests demonstrate the effectiveness of the power control method and the reactive power injection strategy used in this paper in terms of fast response and feasible compliance to the upcoming grid requirements.

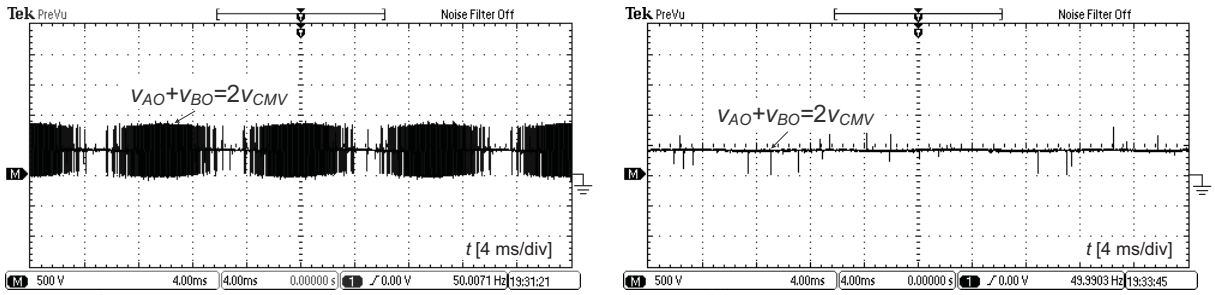

(a) common mode voltage with unipolar modulation (b) common mode voltage with bipolar modulation

Fig. 12. Common mode voltage of a 1 kW full-bridge inverter (DC voltage: 400 V) with different modulation strategies: v_{CMV} [500 V/div].

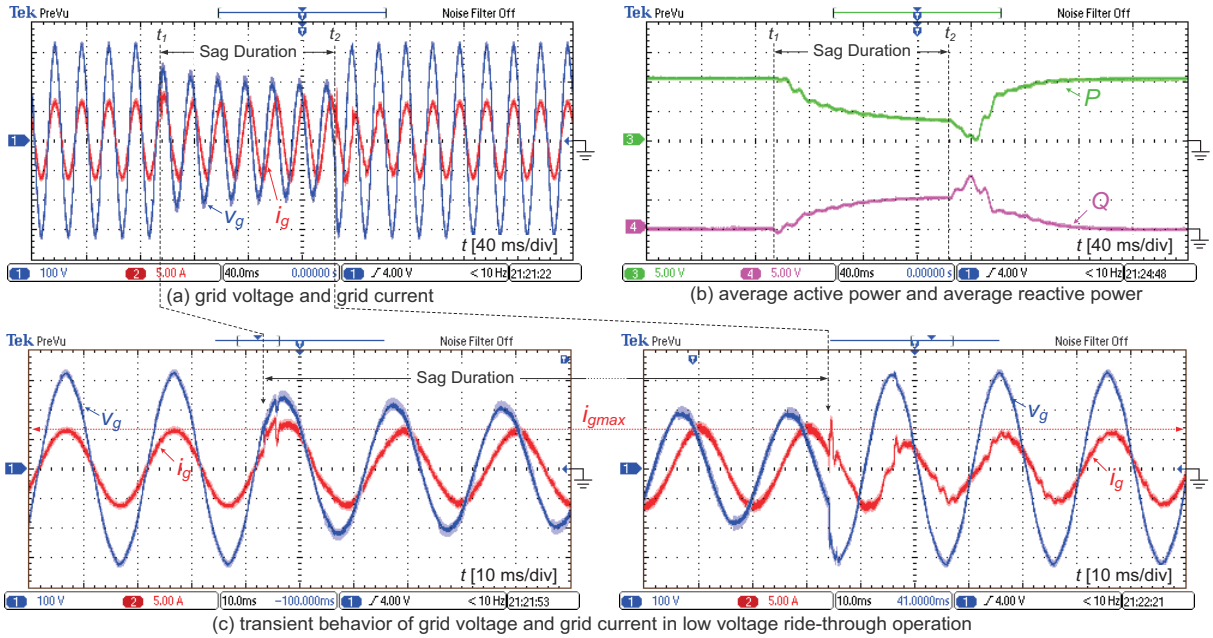

(a) grid voltage and grid current (b) average active power and average reactive power

(c) transient behavior of grid voltage and grid current in low voltage ride-through operation

Fig. 13. Low voltage ride through operation of a 1 kW single-phase full-bridge system with bipolar modulation and constant peak current control strategy (0.43 p.u. voltage sag): (a) grid voltage v_g [100 V/div] and grid current i_g [5 A/div], (b) average active power P [500 W/div] and average reactive power Q [500 Var/div], and (c) transient behavior of grid voltage v_g [100 V/div] and grid current i_g [5 A/div].

V. Conclusions

The LVRT capability of three mainstream single-phase transformerless PV inverters has been explored in this paper. A benchmarking of those inverters has also been presented in terms of efficiency, LVRT capability with reactive power injection, current stresses and leakage current rejection.

With respect to the reactive power injection control, three possibilities have been proposed and discussed. The constant peak current control strategy has been verified by experiments. The results show that the HERIC inverter can achieve a high efficiency, but it is not special suitable for use in the next generation PV systems with LVRT capability or reactive power injection. For this inverter, a possible way to ride-through voltage fault is to modify the modulation scheme during LVRT but at the cost of reducing efficiency. The performance of the FB-DCBP inverter is satisfactory in LVRT operation. It can achieve a slightly higher efficiency compared to the FB-Bipolar topology. However, in LVRT operation, a varying common-mode voltage appears in the FB-DCBP inverter, which may introduce safety problems. Moreover, due to the high switching frequency for the extra devices of the FB-DCBP, high current stresses might appear and further introduce failures to the whole system.

Nevertheless, for different applications, the presented benchmarking result provides a convenient way to select appropriate devices of those inverters. The test results have verified the effectiveness of the single-phase *PQ* control method under grid faults and the constant peak current control strategy for reactive power injection.

References

[1] REN21, "Renewables 2013: Global Status Report (GSR) ," [Online]. Available: http://www.ren21.net/, Jun. 2013.

[2] K.O. Kovanen, "Photovoltaics and power distribution," *Renewable Energy Focus*, vol. 14, no. 3, pp. 20-21, May/Jun. 2013.

[3] Y. Xue, K.C. Divya, G. Griepentrog, M. Liviu, S. Suresh, and M. Manjrekar, "Towards next generation photovoltaic inverters," in *Proc. of ECCE'11*, pp. 2467-2474, 17-22 Sept. 2011.

[4] S.-M. Chen, T.-J. Liang, and K.-R. Hu, "Design, analysis, and implementation of solar power optimizer for DC distribution system," *IEEE Trans. Power Electron.*, vol. 28, no. 4, pp. 1764-1772, Apr. 2013.

[5] P.S. Shenoy, K.A. Kim, B.B. Johnson, and P.T. Krein, "Differential power processing for increased energy production and reliability of

photovoltaic systems," *IEEE Trans. Power Electron.*, vol. 28, no. 6, pp. 2968-2979, Jun. 2013.

[6] E. Koutroulis and F. Blaabjerg, "Design optimization of transformer-less grid-connected PV inverters including reliability," *IEEE Trans. Power Electron.*, vol. 28, no. 1, pp. 325-335, Jan. 2013.

[7] H. Wang, M. Liserre, and F. Blaabjerg, "Toward reliable power electronics: challenges, design tools, and opportunities," *IEEE Ind. Electron. Mag.*, vol. 7, no. 2, pp. 17-26, Jun. 2013.

[8] V. Salas and E. Olías, "Overview of the state of technique for PV inverters used in low voltage grid-connected PV systems: Inverters below 10 kW," *Renewable and Sustainable Energy Reviews*, vol. 13, no. 6–7, pp. 1541-1550, Aug./Sept. 2009.

[9] Y. Yang, F. Blaabjerg, and Z. Zou, "Benchmarking of grid fault modes in single-phase grid-connected photovoltaic systems", *IEEE Trans. Ind. Appl.*, vol. 49, no. 5, in press, Sept./Oct. 2013.

[10] N.P. Papanikolaou, "Low-voltage ride-through concept in flyback inverter-based alternating current- photovoltaic modules," *IET Power Electron.*, vol. 6, no. 7, pp. 1436-1448, Aug. 2013.

[11] T. Neumann, and I. Erlich, "Modelling and control of photovoltaic inverter systems with respect to German grid code requirements," in *Prof. of IEEE PES General Meeting*, pp. 1-8, 22-26 Jul. 2012.

[12] *Grid Code–High and Extra High Voltage*, E. ON GmbH, Bayreuth, Germany, 2006.

[13] R. Teodorescu, M. Liserre, and P. Rodriguez, *Grid converters for photovoltaic and wind power systems*. Wiley - IEEE, 2011.

[14] F. Blaabjerg, R. Teodorescu, M. Liserre, and A.V. Timbus, "Overview of control and grid synchronization for distributed power generation systems," *IEEE Trans. Ind. Electron.*, vol. 53, no. 5, pp. 1398-1409, Oct. 2006.

[15] J. Eloy-Garcia Carrasco, J.M. Tena, D. Ugena, J. Alonso-Martinez, D. Santos-Martin, and S. Arnaltes, "Testing low voltage ride through capabilities of solar inverters," *Electric Power Systems Research*, vol. 96, pp. 111-118, Mar. 2013.

[16] E.J. Coster, J.M.A. Myrzik, B. Kruimer, and W.L. Kling, "Integration issues of distributed generation in distribution grids, " in *Proceedings of the IEEE*, vol. 99, no. 1, pp. 28-39, Jan. 2011.

[17] Y. Yang and F. Blaabjerg, "Low voltage ride-through capability of a single-stage single-phase photovoltaic system connected to the low-voltage grid," *Int'l Journal of Photoenergy*, vol. 2013, 9 papges, 2013. Open Access. Available: http://dx.doi.org/10.1155/2013/257487.

[18] *Reference technical rules for connecting users to the active and passive LV distribution companies of electricity*, Comitato Elettrotecnico Italiano, Italy, 2011.

[19] H. Kobayashi, "Fault ride through requirements and measures of distributed PV systems in Japan," in *Proc. of IEEE PES General Meeting*, pp. 1-6, 22-26 Jul. 2012.

[20] K. Fujii, N. Kanao, T. Yamada, and Y. Okuma, "Fault ride through capability for solar inverters," in *Proc. of EPE'11,* pp. 1-9, 2011.

[21] Y. Bae, T.-K. Vu, and R.-Y. Kim, "Implemental control strategy for grid stabilization of grid-connected PV system based on german grid code in symmetrical low-to-medium voltage network," *IEEE Trans. Energy Convers.*, vol. 28, no. 3, pp. 619-631, Sept. 2013.

[22] Y. Miyamoto, "Technology for high penetration residential PV systems on a distribution line in Japan," in *Proc. of the 5th Int'l Conf. on Integration of Renewable and Distributed Energy Resources,* 4-6 Dec. 2012.

[23] A. Ellis, "PV interconnection in the US: IEEE Standard 1547 Status and Outlook," in *Proc. of the 5th Int'l Conf.on Integration of Renewable and Distributed Energy Resources,* 4-6 Dec. 2012.

[24] S.B. Kjaer, J.K. Pedersen, and F. Blaabjerg, "A review of single-phase grid-connected inverters for photovoltaic modules," *IEEE Trans. Ind. Appl.,* vol. 41, no. 5, pp. 1292-1306, Sept./Oct. 2005.

[25] S.V. Araujo, P. Zacharias, and R. Mallwitz, "Highly efficient single-phase transformerless inverters for grid-connected PV systems," *IEEE Trans. Ind. Electron.*, vol. 57, no. 9, pp. 3118-3128, Sept. 2010.

[26] R. Gonzalez, J. Lopez, P. Sanchis, and L. Marroyo, "Transformerless inverter for single-phase photovoltaic systems," *IEEE Trans. Power Electron.*, vol. 22, no. 2, pp. 693-697, Mar. 2007.

[27] S.R. Gonzalez, C.J. Coloma, P.L. Marroyo, T.J. Lopez, and G.P. Sanchis "Single-phase inverter circuit for conditioning and converting dc electrical energy into ac electrical," International Patent Application, Pub. No. WO/2008/015298, 7 Feb. 2008.

[28] T. Kerekes, R. Teodorescu, P. Rodriguez, G. Vazquez, and E. Aldabas, "A new high-efficiency single-phase transformerless PV inverter topology," *IEEE Trans. Ind. Electron.*, vol. 58, no. 1, pp. 184-191, Jan. 2011.

[29] H. Schmidt, S. Christoph, and J. Ketterer, "Current inverter for direct/alternating currents, has direct and alternating connections with an intermediate power store, a bridge circuit, rectifier diodes and a inductive choke," German Patent DE10 221 592 A1, 4 Dec. 2003.

[30] M. Victor, F. Greizer, S. Bremicker, and U. Hubler, "Method of converting a direct current voltage from a source of direct current voltage, more specifically from a photovoltaic couse of direct current voltage, into a alternating current voltage," US Patent Application, Pub. No. US 2005/0286281 A1, 29 Dec. 2005.

[31] I. Patrao, E. Figueres, F. Gonzalez-Espin, and G. Garcera, "Transformerless topologies for grid-connected single-phase photovoltaic inverters," *Renewable and Sustainable Energy Reviews*, vol. 15, no. 7, pp. 3423-3431, Sept. 2011.

[32] L. Zhang, K. Sun, L. Feng, H. Wu, and Y. Xing, "A family of neutral point clamped full-bridge topologies for transformerless photovoltaic grid-tied inverters," *IEEE Trans. Power Electron.*, vol. 28, no. 2, pp. 730-739, Feb. 2013.

[33] B. Gu, J. Dominic, J.-S. Lai, C.-L. Chen, T. LaBella, and B. Chen, "High reliability and efficiency single-phase transformerless inverter for grid-connected photovoltaic systems," *IEEE Trans. Power Electron.*, vol. 28, no. 5, pp. 2235-2245, May 2013.

[34] S. Saridakis, E. Koutroulis, and F. Blaabjerg, "Optimal design of modern transformerless PV inverter topologies," *IEEE Trans. Energy Convers.*, vol. 28, no. 2, pp. 394-404, Jun. 2013.

[35] B. Ji, J.Wang, and J. Zhao, "High-efficiency single-phase transformer-less PV H6 inverter with hybrid modulation method," *IEEE Trans. Ind. Electron.*, vol. 60, no. 5, pp. 2104-2115, May 2013.

[36] Y. Yang, K. Zhou, and F. Blaabjerg, "Harmonics suppression for single-phase grid-connected PV systems in different operation modes," in *Proc. of APEC'13*, pp. 889-896, 17-21 Mar. 2013.

[37] S.A. Khajehoddin, M. K. Ghartemani, A. Bakhshai, and P. Jain, "A power control method with simple structure and fast dynamic response for single-phase grid-connected DG systems," *IEEE Trans. Power Electron.*, vol. 28, no. 1, pp. 221-233, Jan. 2013.

[38] D.N. Zmood and D.G. Holmes, "Stationary frame current regulation of PWM inverters with zero steady-state error," *IEEE Trans. Power Electron.*, vol. 18, no. 3, pp. 814-822, May 2003.

[39] X. Yuan, W. Merk, H. Stemmler, and J. Allmeling, "Stationary-frame generalized integrators for current control of active power filters with zero steady-state error for current harmonics of concern under unbalanced and distorted operating conditions," *IEEE Trans. Ind. Appl.*, vol. 38, no. 2, pp. 523 –532, Mar./Apr. 2002.

[40] H.-R. Seo, S.-J. Jang, G.-H. Kim, M. Park, and I.-K. Yu, "Hardware based performance analysis of a multi-function single-phase PV-AF system," in *Proc. of ECCE*, , pp. 2213-2217, 20-24 Sept. 2009.

[41] M.T. Haque, "Single-phase PQ theory," in *Proc. of PESC'02* , vol. 4, pp. 1815-1820, 23-27 Jun. 2002.

[42] R. Bojoi, L.R. Limongi, D. Roiu, and A. Tenconi, "Enhanced power quality control strategy for single-phase inverters in distributed generation systems," *IEEE Trans. Power Electron.*, vol. 26, no. 3, pp. 798-806, Mar. 2011.

[43] M. Prodanovic, K. De Brabandere, J. Van Den Keybus, T. Green, and J. Driesen, "Harmonic and reactive power compensation as ancillary services in inverter-based distributed generation," *IET Gener. Transm. Distrib.*, vol. 1, no. 3, pp. 432-438, May 2007.

[44] M. Saitou and T. Shimizu, "Generalized theory of instantaneous active and reactive powers in single-phase circuits based on Hilbert transform," in *Proc. of PESC*, vol. 3, pp. 1419-1424, 2002.

[45] M. Ciobotaru, R. Teodorescu, and F. Blaabjerg, "A new single-phase PLL structure based on second order generalized integrator," in *Proc. of PESC*, pp. 1-6, 18-22 Jun. 2006.

[46] S. Shinnaka, "A robust single-phase PLL system with stable and fast tracking," *IEEE Trans. Ind. Appl.*, vol. 44, no. 2, pp. 624-633, Mar./Apr. 2008.

[47] R.A. Mastromauro, M. Liserre, T. Kerekes, and A. Dell'Aquila, "A single-phase voltage-controlled grid-connected photovoltaic system with power quality conditioner functionality," *IEEE Trans. Ind. Electron.*, vol. 56, no. 11, pp. 4436-4444, Nov. 2009.

[48] R. Majumder, "Reactive power compensation in single-phase operation of microgrid," *IEEE Trans. Ind. Electron.*, vol. 60, no. 4, pp. 1403-1416, Apr. 2013.

[49] Y.-S. Wu, C.-H. Chang, Y.-M. Chen, C.-S. Cheng, C.-W. Liu, and Y.-R. Chang, "The current control of PV inverter for low voltage ride through," in *Proc. of EPE/PEMC*, pp. LS1d.4-1-LS1d.4-6, Sept. 2012.

[50] P. Rodriguez, A.V. Timbus, R. Teodorescu, M. Liserre, and F. Blaabjerg, "Flexible active power control of distributed power generation systems during grid faults," *IEEE Trans. Ind. Electron.*, vol. 54, no. 5, pp. 2583-2592, Oct. 2007.
[51] M.S. El Moursi, W. Xiao, and J.L. Kirtley, "Fault ride through capability for grid interfacing large scale PV power plants," *IET Gener. Transm. Distrib.,* , vol. 7, no. 9, pp. 1027-1035, Sept. 2013.
[52] G.M.S. Azevedo, G. Vazquez, A. Luna, D. Aguilar, and A. Rolan, "Photovoltaic inverters with fault ride-through Capability," in *Proc. of ISIE'09*, pp. 549-553, 5-8 Jul. 2009.
[53] C.H. Benz, W.-T. Franke, and F.W. Fuchs, "Low voltage ride through capability of a 5 kW grid-tied solar inverter," in *Proc. of EPE/PEMC*, pp. T12-13-T12-20, 6-8 Sept. 2010.
[54] X. Bao, P. Tan, F. Zhuo, and X. Yue, "Low voltage ride through control strategy for high-power grid-connected photovoltaic inverter," in *Proc. of APEC'13*, pp. 97-100, 17-21 Mar. 2013.
[55] H.-C. Chen, C.-T. Lee, P.T. Cheng, R.Teodorescu, F. Blaabjerg, and S. Bhattacharya, "A flexible low-voltage ride-through operation for the distributed generation converters," in *Proc. of PEDS'13*, pp. 1354-1359, 22-25 Apr. 2013.
[56] K. Ma, M. Liserre, and F. Blaabjerg, "Power controllability of three-phase converter with unbalanced AC source," in *Proc. of APEC'13*, pp. 342-350, 17-21 Mar. 2013.
[57] Y. Yang and F. Blaabjerg, "A new power calculation method for single-phase grid-connected systems," in *Proc. of ISIE'13*, pp. 1-6, 28-31 May 2013.
[58] S. Saridakis, E. Koutroulis, and F. Blaabjerg, "Optimal design of modern transformerless PV inverter topologies," *IEEE Trans. Energy Convers.*, vol. 28, no. 2, pp. 394-404, Jun. 2013.

Frede Blaabjerg (S'86-M'88-SM'97-F'03) received the Ph.D. degree from Aalborg University, Aalborg Denmark, in 1992.

Hw was with ABB Scandia, Randers, Denmark, from 1987 to 1988. He became an Assistant Professor in 1992 and then an Associate Professor in 1996 at Aalborg University, where he has been a Full Professor in power electronics and drives since 1998. He has been a part-time Research Leader with the Research Center Risoe working with wind turbines. In 2006-2010, he was the Dean of the Faculty of Engineering, Science and Medicine and became a Visiting Professor with Zhejiang University, Hangzhou China, in 2009. His research areas are in power electronics and its applications such as wind turbines, photovoltaic systems, and adjustable speed drives.

Dr. Blaabjerg has been the Editor-in-Chief of the IEEE TRANSACTIONS ON POWER ELECTRONICS in 2006-2012. He was a Distinguished Lecturer of the IEEE Power Electronics Society (PELS) from 2005 to 2007 and of the IEEE Industry Applications Society from 2010 to 2011. He was the recipient of the 1995 Angelos Award for his contributions to modulation technique and the Annual Teacher Prize at Aalborg University. In 1998, he also received the Outstanding Young Power Electronics Engineer Award from the IEEE PELS. He has received more than ten IEEE prize paper awards and another prize paper award at PELINCEC Poland 2005. He received the IEEE PELS Distinguished Service Award in 2009 and the EPE-PEMC 2010 Council award.

Yongheng Yang (S'12) received the B.Eng. degree in Electrical Engineering and Automation from Northwestern Polytechnical University, Xi'an, China, in 2009. During 2009 – 2011, he was enrolled in a master-doctoral program in the School of Electrical Engineering at Southeast University, Nanjing, China. In that period, he has been doing with the modeling and control of single-phase grid-connected photovoltaic (PV) systems. From March to May in 2013, he was a visiting scholar in the Department of Electrical and Computer Engineering at Texas A&M University, College Station, TX, USA. He is currently working towards the Ph.D. degree in the Department of Energy Technology at Aalborg University, Aalborg East, Denmark.

His research interests include grid detection, synchronization, and control of single-phase grid-connected PV systems in different operation modes, and the reliability for the next generation PV inverters.

Huai Wang (S'07-M'12) received the B.Eng. degree in Electrical and Electronic Engineering from Huazhong University of Science and Technology, Wuhan, China, in 2007, and the Ph.D. degree in Electronic Engineering from City University of Hong Kong, Kowloon, Hong Kong, in 2012.

Since 2012, he has been with Aalborg University, Denmark, where he is currently an Assistant Professor in the Department of Energy Technology, working at the Center of Reliable Power Electronics (CORPE). From September to November 2013, he was a visiting scientist at Massachusetts Institute of Technology (MIT), USA. From April to September 2010, he was an intern student at ABB Corporate Research Center, Switzerland. He has authored or coauthored more than 30 technical papers and filed 3 patents. His research interests include reliability of capacitors for dc-link application, reliability of power electronic systems, high-voltage dc-dc power converters, fast dynamic control of converters, and passive components reduction technology.

Dr. Wang is the recipient of several paper awards and project awards from industry, the IEEE and the Hong Kong Institution of Engineers (HKIE). He is currently a committee member of the IEEE Power Electronics Society Technical Committee on High Performance Emerging Technologies.